Desalination and Water Treatment
www.deswater.com

doi: 10.5004/dwt.2019.24694

170 (2019) 199–210
December

Application of polyaniline/activated carbon nanocomposites derived from different agriculture wastes for the removal of Pb(II) from aqueous media

Somaia G. Mohammad[a,*], Dalia E. Abulyazied[b], Sahar M. Ahmed[b]

[a]*Central Agricultural Pesticides Laboratory, Pesticide Residues and Environmental Pollution Department, Agriculture Research Center (ARC), 12618, Dokki, Giza, Egypt, Fax: +203 7602209; emails: somaiagaber@yahoo.com/ sommohammad2015@gmail.com*
[b]*Petrochemical Department, Egyptian Petroleum Research Institute, Ahmed El-Zomor St., Nasr City, Cairo, Egypt, Fax: +20 2 2274 7433; emails: daliaelsawy@hotmail.com (D.E. Abulyazied), saharahmed92@hotmail.com (S.M. Ahmed)*

Received 3 August 2016; Accepted 10 July 2019

ABSTRACT

Polyaniline/agricultural waste activated carbon (PANI/AC) composites were prepared by chemical oxidative polymerization of aniline monomer with activated carbon obtained from different sources of agricultural wastes present in the environment. The prepared PANI/AC composites were characterized by Fourier transform infrared spectroscopy, X-ray diffraction, scanning electron microscopy, transmission electron microscopy and Brunauer–Emmett–Teller surface area for the removal of lead ions by polyaniline/activated carbon nanocomposites. The thermal stability of the different composites was determined by thermogravimetric analysis. As well as, the electrical conductivity was measured for the prepared composites. The effect of different pH and the adsorbent dose of the composites on the removal of the lead ion from aqueous solution was studied. Results showed that the adsorption maximum occurs at around pH 4.0; adsorption equilibrium was achieved in 90 min at 20 mg L^{-1} Pb(II) concentration and adsorbent dose 1 g/100 mL for each composite. Removal of Pb(II) ions increases with increasing solution pH and pH maximum value was at pH 4 for all the composites. By comparing the removal efficiency between polyaniline, polyaniline/orange peels activated carbon, polyaniline/peach stones activated carbon, polyaniline/banana peels activated carbon, polyaniline/apricot stones activated carbon and polyaniline/pomegranate peels activated carbon for the removal of lead ions, the removal efficiency of polyaniline/orange peels activated carbon nanocomposite is higher than the other composites. The maximum adsorption capacity of PANI/OPAC nanocomposite was 6.81 mg g^{-1}. The thermal stability and the electrical conductivity of the composites were enhanced with different agricultural sources of activated carbon. The experimental equilibrium biosorption data were analyzed by Freundlich and Langmuir isotherm models. The Freundlich isotherm provided a better fit than Langmuir isotherm. The results indicated that the adsorption of Pb(II) by PANI/OPAC follows pseudo-second-order kinetic model. The thermodynamics indicated that the process is endothermic and spontaneous. Desorption experiments were carried out by different desorbing agents such as distilled water, EDTA and HCl. They found that the desorption using 0.1 M HCl is the most effective desorbing agent.

Keywords: Polyaniline; Agricultural wastes; Activated carbons; Composites; Lead ions; Aqueous media

* Corresponding author.

1. Introduction

Wastewater and surface water containing heavy metal is becoming a severe environmental and public health problem. Lead is the most common metal contaminant in wastewater which is discharged by industrial processing methods such as electroplating, alloying, pigmenting, plastic manufacturing, mining, metallurgy and refining [1]. Lead disperses throughout the body immediately and causes harmful effects. It can damage the red blood cells and limit their ability to carry oxygen to the organs and tissues. It can also cause a range of physiological disorders such as headache, hearing problems, learning disabilities, behavioral problems, brain damages even causes' death [2].

The maximum concentration of lead in drinking water is 0.1–0.05 mg L^{-1} as recommended by the World Health Organization (WHO) [3]. So, it is very important to remove lead ions from the water before they are released to the environment. Removal of lead from wastewater by conventional methods such as membrane filtration, chemical precipitation, ion-exchange, chelation, reverse osmosis, solvent extraction, evaporation and electroplating [4]. However, these methods proved either inefficient or expensive in case of low concentration (1–100 mg L^{-1}) of heavy metals prevailing in the environment [5].

Biosorption proved to be an alternate method that is effective, economic as well as environment friendly. There are several different types of agricultural by-products that have been used for activated carbon (AC) production at the laboratory or an industrial level including, apricot stones, banana and pomegranate peels [6,7]. The use of different materials as precursors for the preparation of activated carbon not only produces useful adsorbents for the purification of contaminated environments but also contributes to minimizing the undesirable solid wastes.

Polyaniline (PANI) is one of the most environmentally stable known conducting polymer due to its high electrical conductivity and ease of preparation [8].

Many researchers have examined polyaniline (PANI) and polypyrrole (PPy) as an adsorbent for the removal of heavy metal ions and dyes from aqueous solution [9–22]. The presence of large amounts of amine (–NH) groups in the polymer makes it a suitable candidate for the removal of heavy metals. Many modifications for polyaniline and polypyrrole have been made to increase the sorption capacity and also make it into more processable in the water treatment process [23–27].

The main purpose of this paper is the preparation of polyaniline/activated carbon composites from different agricultural wastes as green environmentally friendly adsorbents to remove the lead ions from aqueous solution. The adsorbents used in this work were prepared in a laboratory scale from banana peels (BPAC), orange peels (OPAC) and pomegranate peels (PPAC) besides peach stones (PSAC) and apricot stones (ASAC) via chemical activation using phosphoric acid as an activating agent. The PANI/AC composites were synthesized by using in-situ polymerization, these composites were ground to nanoscale using mechanical ball mill to give PANI/ACs nanocomposites. Moreover, the thermal stability and the electrical conductivity of these composites were measured.

2. Experimental

2.1. Materials and methods

All reagents were used without further purification. Distilled deionized water was used throughout this work. A stock solution of Pb(II) (1,000 mg L^{-1}) was prepared in milli-Q water with $Pb(NO_3)_2$. It was then diluted to prepare solutions of the desired concentrations. The pH of the solution was monitored by adding 0.5 M HCl and 0.5 M NaOH solution as per the required pH value. Aniline and ammonium peroxydisulfate are purchased from Sigma-Aldrich (St. Loius, MO, USA).

2.2. Preparation of different eco-friendly activated carbon from agricultural wastes

The waste peels of banana, orange, pomegranate beside peach and apricot stone wastes (collected from the local market in Egypt) were first washed with double distilled water and dried in an oven at 80°C overnight.

Chemical activation of the adsorbents was carried out by orthophosphoric acid because it is popular, environment-friendly and can be easily removed during washing of the activated carbon [28].

The adsorbents were then soaked in orthophosphoric acid (H_3PO_4) with an impregnation ratio of 1:1 (w/w) for 24 h and dehydrated in an oven overnight at 105°C. The samples were activated in a closed muffle furnace to increase the surface area at 500°C for 2 h. The AC_s produced was cooled to room temperature and washed with 0.1 M HCl and successively with distilled water. Washing with distilled water was done repeatedly until the pH of the filtrate reached 6–7. The final products were dried in an oven at 105°C for 24 h and stored in vacuum desiccators until needed [29].

2.3. Polyaniline/activated carbon composites preparation

PANI/AC composites were synthesized (Fig. 1) by in situ polymerization of aniline with ammonium peroxydisulfate (APS) as the oxidant in the presence of AC particles (5 wt.%). A solution of HCl (1 M, 60 mL) containing AC (0.465 g) was sonicated at room temperature to disperse the AC particles for 30 min. Aniline monomer (9.3 g) was then added to the AC suspension and stirred for 30 min. A solution of HCl (1 M, 60 mL) containing APS (22.8 g) was added dropwise to the well-stirred reaction mixture over 1 h. After a few minutes, the dark suspension became green, indicating polymerization of aniline; polymerization was carried out at 0°C and stirring for 24 h. The composites

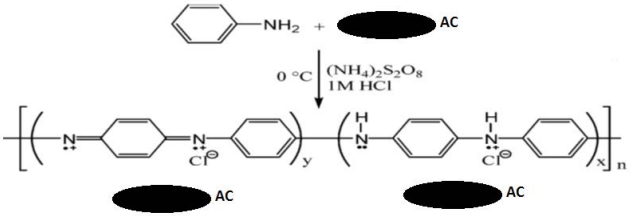

Fig. 1. Preparation of polyaniline nanocomposite.

were obtained by filtering and washing the reaction mixtures with deionized water, resulting in the conductive salt form of the PANI/AC composites. The composites were isolated by vacuum filtration and washed with deionized water [30].

The PANI/AC composites were abbreviated as PANI/BPAC, PANI/OPAC, PANI/PPAC, PANI/PSAC and PANI/ASAC. The adsorbents were ground to nanoscale using mechanical ball mill RWTCH Planetary Ball mill type (RM400).

2.4. Determination of lead ions

The concentration of lead ions measured by inductively coupled plasma with atomic emission spectroscopy (ICP–AES). The sorption capacity was determined by using the following equation, considering the concentration difference of the solution at the beginning and equilibrium [31].

$$q_e = \frac{\left(C_0 - C_e\right)V}{m} \tag{1}$$

where C_0 and C_e are the initial and the equilibrium concentrations in mg L^{-1}, respectively, V is the volume of solution (mL) and m is the amount of adsorbent used (g). The efficiency of Pb(II) from solution was calculated by the following equation:

$$\text{Removal efficiency}\left(\%\right) = \frac{\left(C_0 - C_e\right)}{C_0} \times 100 \tag{2}$$

2.4.1. Desorption and regeneration study

To study the possibility of repeated use of the adsorbent, desorption and regeneration experiments were carried out for PANI/OPAC. Desorption studies help in determining the recovery of the adsorbent and adsorbate, protect the environment and recycling of the adsorbent.

After adsorption experiments with 20 mg L^{-1} solution of Pb(II) ions and 1 g of PANI/OPAC nanocomposite. The use of PANI/OPAC was regenerated with different desorbing agents such as distilled water, 0.1 M EDTA and 0.1 M HCl for 2 h at room temperature. After desorption experiments, samples were analyzed by ICP–AES as before. The regeneration was repeated for several cycles to determine the reusability of the adsorbent used.

2.5. Characterization of PANI/AC composites

2.5.1. Fourier-transform infrared analysis

Polyaniline/ACs composites were analyzed by Fourier transform infrared (FTIR) on PerkinElmer 1720 (940 Winter, Waltham, MA 02451, USA).

2.5.2. X-ray diffraction analysis

X-ray diffraction (XRD) measurements were performed on X'Pert Pro diffractometer with Cu Kα radiation (λ = 0.154 nm, 45 kV and 30 mA) at room temperature (25°C).

2.5.3. Scanning electron microscope

The surface morphology of the prepared composites was performed by a scanning electron microscopy (SEM) (JEOL 5400), at 30 kV accelerated voltage. Before scanning, each adsorbent was coated with a thin layer of gold using a sputter coater to make it conductive.

2.5.4. Transmission electron microscopy

Transmission electron microscopy micrographs of PANI/OPAC nanocomposite were carried out by (TEM; product name: JX1230; manufactured by JEOL [Japan]) with micro-analyzer electron probe.

2.5.5. BET surface area

The BET surface area of PANI/OPAC nanocomposite was determined by a low-temperature N_2 gas adsorption–desorption technique using AUTOSORB-1 surface area and pore size analyzer at 77 K.

2.5.6. Electrical conductivity

The electrical conduction was performed using the two electrode method at room temperature. Impedance measurements were performed on GW Instek LCR-811OG in the frequency ranging from 20 Hz to 10 MHz at room temperature.

3. Result and discussion

3.1. FTIR of the composites

The FTIR spectra for PANI and PANI/ACs (prepared in situ) composites are shown in Fig. 2. The base form of PANI has several important peaks in the FTIR (Fig. 2a) (PANI). The characteristic sharp band at 1,119 cm^{-1} was due to C–N tertiary aromatic vibrations. The band at 1,301 cm^{-1} was due to C–N primary and secondary vibrations. The broad band at 3,450–3,200 cm^{-1} was due to the single-bridge compound polymeric association or to NH stretching vibrations. The bands at 1,567 and 1,478 cm^{-1} were due to the presence of the quinoid structure, and the band at 1,242 cm^{-1} was due to the C–N stretching mode for the benzenoid ring. The band at 810 $cm^{-1}$was attributed to the out-of-plane bending vibrations of C–H on the para-substituted aromatic ring.

The FTIR spectra of PANI/ACs composites are shown in Fig. 2. The characteristic peaks of PANI can be seen in all these composite spectra, with a little shift due to the formation of a covalent bond between the C atoms of AC particles, and the C atoms of aromatic rings in the polymer backbone structure or N atoms on the exterior aromatic rings of the polymer chains. Also, the addition of AC particles caused reductions in the intensity of the aromatic ring deformation peak at 508 cm^{-1}. This indicates that the aromatic rings on the polymer structure have become more stable.

The FTIR spectra were obtained for polyaniline/activated carbon nanocomposites before (a) and after Pb(II) ions biosorption process (b) (Fig. 2). The results showed that activated carbons have different functional groups such as amide, hydroxyl and carboxyl. Some of these functional

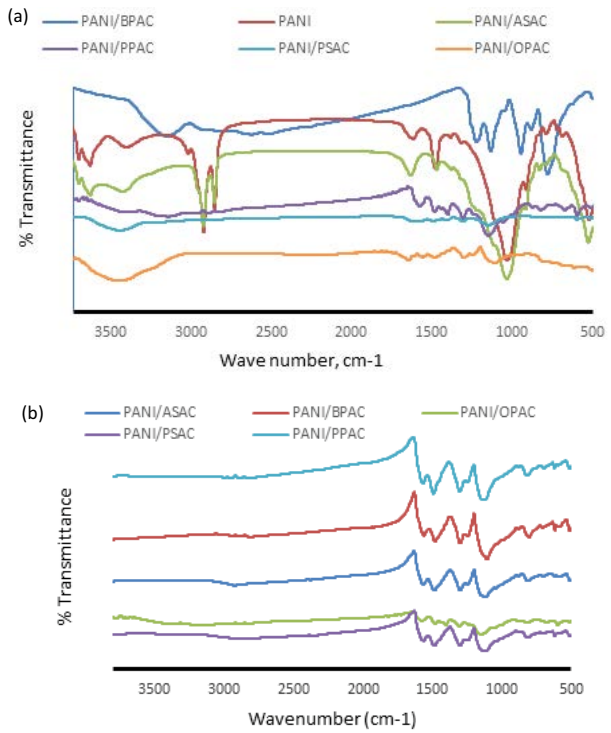

Fig. 2. FTIR of (a) before and (b) after adsorption of Pb(II) ions by PANI/ACs nanocomposites.

groups changed after the biosorption process. The comparisons of the FTIR spectra of nanocomposites before and after Pb(II) biosorption give the following bands and peaks. The bands at 3,419.22 and 3,454.93 cm^{-1} are the OH stretching of polymeric compounds. The bands located at 1,376.17 and 1,591.84 cm^{-1} are possibly due to the functional groups such as C=O in carboxylic groups and carboxylate moieties. The additional small peaks at 1,090.55 cm^{-1}. The band at 1,622.02 cm^{-1} corresponds to carbonyl stretching vibration of amide considered to be due to the combined effect of double-bond stretching vibration and –NH deformation band for Pb(II)-loaded activated carbon. The C=O functional groups have been reported to show very high coordination with trace metals; hence it disappeared in the Pb(II)-loaded activated carbon. For this reason, the presence of these functional groups may be responsible for good adsorptive behavior of the activated carbon toward the Pb(II) ions.

Among the functional groups, amine, carboxylic acid and hydroxyl have been proposed to be responsible for the adsorption of heavy metal ions on the cell surfaces of adsorbent. Li et al. [32] had reported that the functional groups, such as amine, carboxylic acid and hydroxyl, are responsible for the adsorption of heavy metal ions on the cell surfaces of the adsorbent.

3.1.2. Mechanism of adsorption

The possible mechanism of adsorption of Pb(II) onto polyaniline with different activated carbon nanocomposites is shown in Fig. 3. Kanwal et al. [33] reported that the nitrogen-containing functional groups can act as adsorption sites for metal ions, besides the functional groups, carboxylic acid and hydroxyl groups present in the activated carbon as mentioned before in FTIR.

3.1.3. X-ray diffraction

The XRD pattern of the polyaniline/activated carbon composites is shown in Fig. 4. The XRD patterns of the prepared PANI and the prepared PANI/AC composites exhibited sharp peaks at 2θ = 21° and 25° this indicated the presence of high crystallinity and condensed structure of polyaniline. The peak centered at 2θ = 25° was ascribed to the periodicity parallel to the polymer chain, and the latter peak may have been caused by the periodicity to the polymer chain. In the prepared PANI/AC composites, there is an appearance of peaks at 2θ = 26° and 45° corresponding to d_{002} and d_{100}, respectively. These peaks belong to the turbostratic structure (graphite-like microcrystallites). The turbostratic model assumes that the samples are made of graphite-like microcrystallites, bounded by the cross-linking network, consisting of several graphite-like layers, stacked nearly parallel and equidistant, with each layer having a random orientation reported by Kumar et al. [34].

3.1.4. SEM of the composites

Fig. 5 shows the SEM images of PANI and the PANI/AC composites (b-f). SEM was used to examine the surface structure of PANI/AC composites. In Fig. 5, images of PANI and PANI/AC composites are shown (magnification at 1,000×

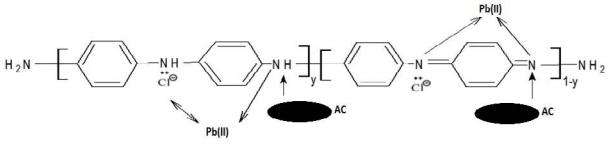

Fig. 3. Schematic diagram of mechanism of Pb(II) adsorption on PANI/ACs nanocomposites.

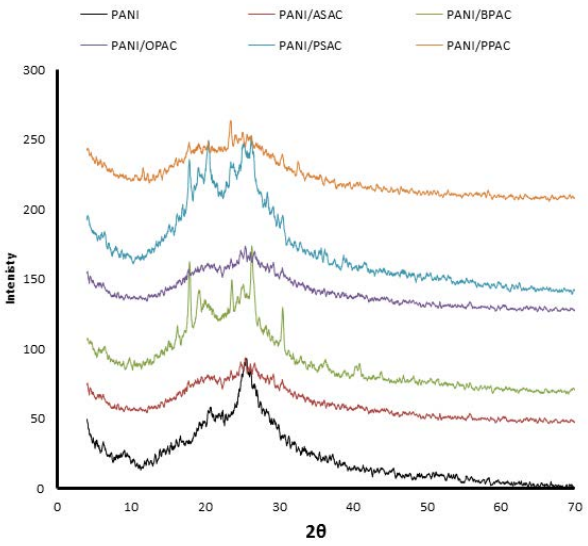

Fig. 4. XRD of PANI and PANI/ACs composites.

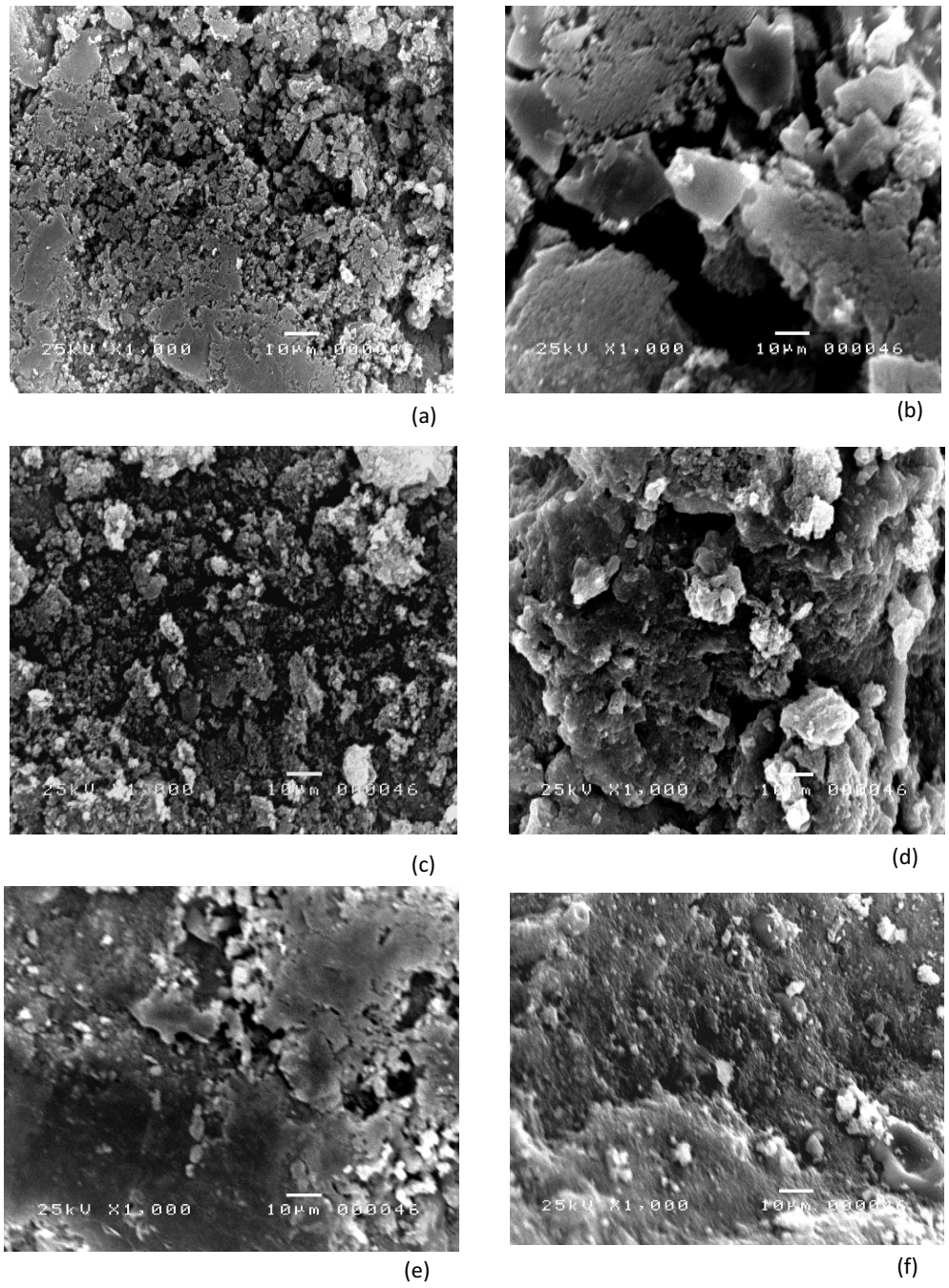

Fig. 5. SEM of (a) PANI, (b) PANI/PPAC, (c) PANI/OPAC, (d) PANI/BPA, (e) PANI/PSAC and (f) PANI/ASAC.

and an accelerating voltage of 30 kV). From the images, smooth marks are observed on the fractured surface. AC particles are attached well on the surface of the PANI and good distributed, where the AC in PANI was being pulled out of the PANI matrix consequently, it is confirmed that interfacial bonding was enhanced. The uniform dispersion of small particles is observed for AC coming from orange peels activated carbon (PANI/OPAC), it is optimal for the adsorbent surface as this can provide more reactive sites for the reactants than aggregated particles. At 1,000× such magnification, SEM micrographs revealed that wide varieties of pores are present in activated carbon. In the case of AC from apricot and peach stones, it is also found that there are holes and caves type openings on the surface of the adsorbent, which would have more surface area available for adsorption.

3.1.5. Transmission electron microscopy

The results of the PANI/OPAC nanocomposite are presented in Fig. 6. Based on the TEM study, the presence of darkened areas on the surface of PANI is due to the loading

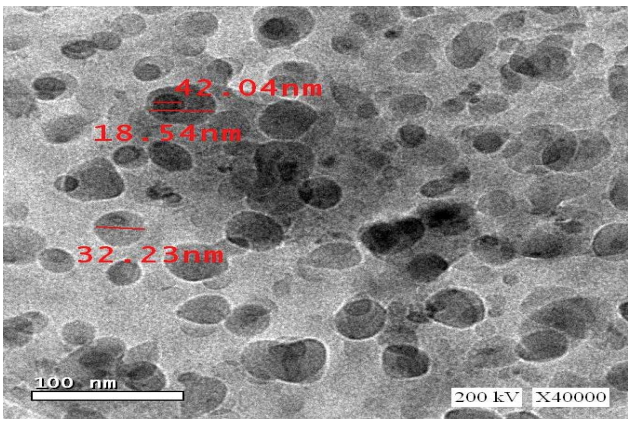

Fig. 6. TEM of PANI/OPAC nanocomposite.

of AC particles. The particle size lies in the range of 15–45 nm, hence the synthesized PANI/OPAC is nanocomposite (Fig. 6).

3.1.6. BET surface area

The surface area and porosity of PANI/OPAC that were analyzed by Brunauer–Emmett–Teller (BET) method also greatly affect their Pb(II) adsorption capacities. The International Union of Pure and Applied Chemistry (IUPAC) recommended the classification of materials based on their total porosity. Accordingly, adsorbents can be divided into three categories, namely macropores ($d > 50$ nm), mesopores ($2 < d < 50$ nm) and micropores ($d < 2$ nm) [35]. The N_2 adsorption–desorption isotherms of PANI/OPAC before and after Pb(II) adsorption are shown in Figs. 7a and b. The unloaded PANI/OPAC has a surface area of 119 m^2 g^{-1}, however,

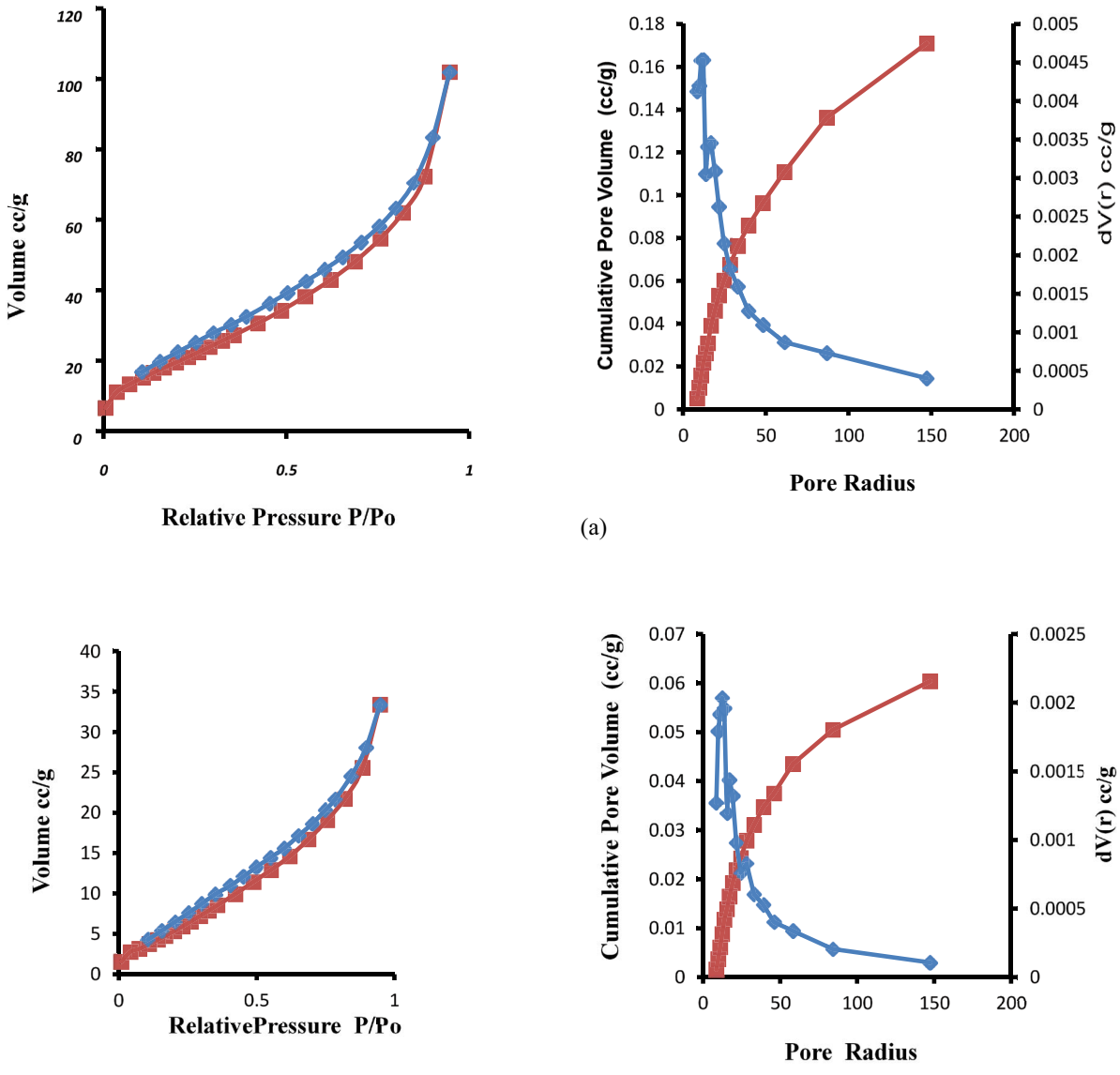

Fig. 7. Adsorption/desorption isotherms of N_2 and size distribution for PANI/OPAC before (a) and after (b) adsorption of Pb(II).

incorporation of Pb(II) has decreased this area significantly to 46.8 m^2 g^{-1}, the decrease in the BET surface area can be attributed to the loading of a significant portion of the micropores of PANI/OPAC with Pb(II) particles during adsorption. It can be seen that the OPAC possesses large amounts of micropores in its structures and the pores disappeared after Pb(II) adsorption, which could be regarded as evidence of the micropore occupation by Pb(II) ions [36]. On the other hand, the pore size distribution of the investigated PANI/OPAC has been calculated and presented in Table 1.

3.1.7. Thermal stability

The thermal stability of the PANI and PANI/AC composites was determined from the TGA thermogram (Fig. 8). It is clear from the figure that all the curves show the thermal decomposition of the PANI and its composites with different ACs occurred through two different weight loss steps. The initial weight loss below 150°C was attributed to the evaporation of moisture adsorbed and the other volatile matter retained in the composite system. The second major weight loss was observed at around 245°C, which might be due to the removal of higher oligomers of PANI. The third major weight loss approximately around 476°C was attributed to the thermo-oxidative decomposition of PANI resulting in various degradation products, such as ammonia, aniline, methane, acetylene, etc. [37]. The decomposition temperatures of all samples at 5% and 10% loss of the weight were showed in Table 2. The data indicate the enhancement of the thermal stability of PANI/AC composites than pure PANI, where the decomposition temperatures at 10 wt% loss for PANI/ASAC, PANI/BPAC, PANI/OPAC, PANI/PSAC and PANI/PPAC increased by 81°C, 75°C, 2°C, 4°C and 56°C, respectively, than the PANI. As well as, the temperatures at maximum loss increased by 18°C, 51°C, 16°C, and 65°C, respectively than the PANI. According to X-ray data, the different metals contained in the different sources of activated carbons resulted in different thermal stabilities of the composites.

3.1.8. Electrical conductivity measurements

The electrical conductivity of the prepared PANI and the prepared PANI/ACs composites was measured at room temperature (Fig. 9). From the plot, it is shown that the electrical conductivity of the PANI sample has the lowest value of the conductivity (3.4771E-07 S cm^{-1}) than that of the composites. PANI can be considered as a fairly good electron donor, so a charge transfer from the quinoid unit of PANI to the AC particles results in an enhancement of the conductivity of the composites [38].

Table 1
Surface area parameters for PANI/OPAC nanocomposite before and after adsorption with Pb(II)

Parameter	PANI/OPAC before adsorption with Pb(II)	PANI/OPAC after adsorption with Pb(II)
Surface area (m^3 g^{-1})	119.028	46.863
Pore volume (cc g^{-1})	0.171	0.06
Pore radius (nm)	12.304	12.297

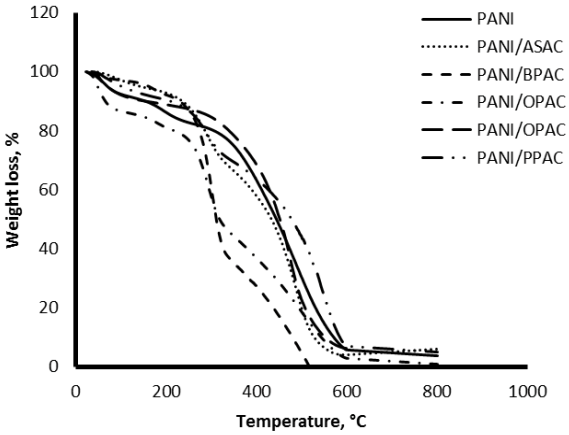

Fig. 8. TGA of PANI and PANI/ACs nanocomposites.

Table 2
Decomposition temperatures of the samples at 10% and maximum loss of the weight

Composites	T_{10}	T_{max}
PANI	154	467
PANI/ASAC	235	485
PANI/BPAC	229	518
PANI/OPAC	158	483
PANI/PSAC	155	532
PANI/PPAC	210	478

3.2. Effect of adsorbent dose

To assess the effect of adsorbent dose, different amounts (0.3–2.0 g) of PANI and PANI/ACs composites were suspended in 100 mL Pb(II) solution (20 mg L^{-1}) at pH 4.0 and contact time. The effect of adsorbent dose on the removal efficiency is shown in Fig. 10. When the adsorbent dose was increased from 0.3 to 1.0 g, the percentage of Pb(II) ions adsorption increased from 10.80 to 20.5, 75.05 to 83.00, 45.80 to 80.23, 55.10 to 74.40, 54.75 to 74.40 and 53.0 to 70.25 for PANI, PANI/OPAC, PANI/PSAC, PANI/BPAC, PANI/ASAC and PANI/PPAC composites, respectively. The removal efficiency of PANI/OPAC is higher than the other composites. There was a non-significant increase in the removal of percentages of Pb(II) when adsorbent dose increases beyond 1.0 g. This suggests that after a certain dose of biosorbent, the maximum adsorption is attained and hence the amount of ions remains constant even with the further addition of a dose of the adsorbent. This is due to an increase in the surface area of the biosorbent, which in turn increases the number of binding sites. Results indicated that the removal efficiency of the PANI/OPAC nanocomposite is higher than the other composites. Similar trends were observed in different adsorbents [39,40].

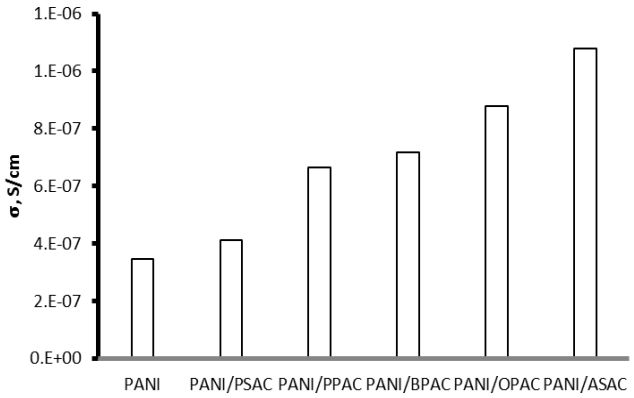

Fig. 9. Electrical conductivity values of PANI and PANI/ACs nanocomposites.

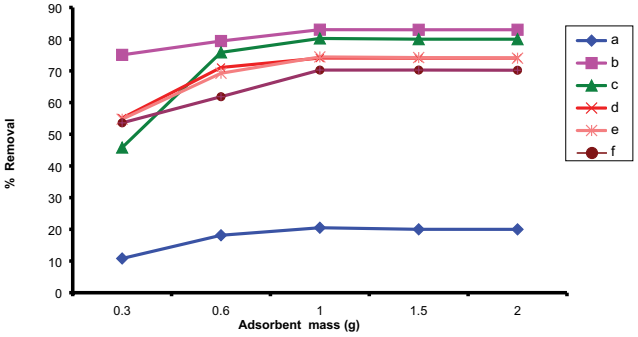

Fig. 10. Effect of adsorbent dose on the removal efficiency with: (a) PANI, (b) PANI/OPAC, (c) PANI/PSAC, (d) PANI/BPAC, (e) PANI/ASAC and (f) PANI/PPAC (initial concentration, contact time, and volume of solution was 20 mg L^{-1}, 2 h, 100 mL, respectively).

3.3. Effect of pH

The pH value of the aqueous solution is an important controlling parameter in the adsorption process. These pH values affect the surface charge of adsorbent, the degree of ionization and speciation of adsorbate during adsorption. To evaluate the influence of this parameter on the adsorption, the experiments were carried out at different initial pH in acidic medium ranging from 2 to 6. The experiment was performed by PANI, PANI/PPAC, PANI/OPAC, PANI/BPAC, PANI/PSAC and PANI/ASAC composites, with an initial lead ions concentration of 20 mg L^{-1} containing 1 g/100 mL at room temperature with a contact time of 2 h. In acidic medium, the concentration of H^+ ions was high. This leads to the development of positive charge on the active sites of biomass and also a competition between Pb(II) ions and H^+ in the bulk of solution to attach with the active binding sites of composites. The results are shown in Fig. 11. Removal of lead increases with increasing solution pH and the maximum value was reached at an equilibrium pH at 4. As we can see in Fig. 4, the removal efficiency of PANI/OPAC was higher than the other composites. So, there were a minimum binding of Pb(II) ions at pH = 4. As the pH of a solution increases, composites become less positive and the concentration of H^+ ions also decreases. Thus, there is less competition of Pb(II) ions with H^+ ions and this resulted in more biosorption [41]. So, it was concluded that the optimum pH for biosorption of Pb(II) ion on different PANI/AC composites was 4.0.

3.4. Effect of contact time

The effect of contact time on the removal of Pb(II) by PANI/OPAC is shown in Fig. 12. The removal of Pb(II) was rapid for the first 10 min and equilibrium was reached within 90 min. Therefore, the period of 90 min was considered the optimum time.

3.5. Adsorption isotherm

To evaluate the adsorption capacity of Pb(II) by PANI/OPAC, isotherms data were tested with two commonly used isotherm models, Langmuir [42] and Freundlich [43] isotherm models.

3.5.1. Langmuir isotherm model

The Langmuir isotherm model is based on the assumption of monolayer adsorption onto the surface containing number of identical sorption sites and no interaction between them [44].

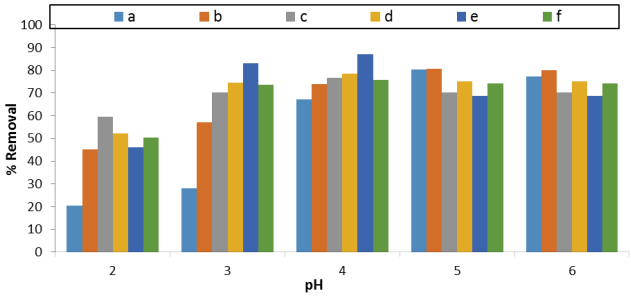

Fig. 11. Effect of pH on the removal efficiency with: (a) PANI, (b) PANI/OPAC, (c) PANI/PSAC, (d) PANI/BPAC, (e) PANI/ASAC and (f) PANI/PPAC (initial concentration, contact time, volume of solution and amount of adsorbent was 20 mg L^{-1}, 2 h, 100 mL and 1 g, respectively).

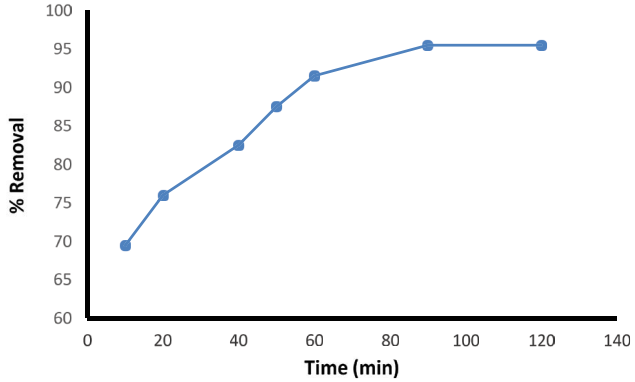

Fig. 12. Effect of contact time for removal of Pb(II) by PANI/OPAC nanocomposite.

The linear form of Langmuir equation is represented by Eq. (3) as follows:

$$\frac{C_e}{q_e} = \frac{1}{Q_m b} + \frac{C_e}{Q_m} \tag{3}$$

3.5.2. Freundlich isotherm model

The Freundlich isotherm is an empirical equation based on the assumption that adsorption occurs on a heterogeneous adsorption surface with different adsorption energies [45].

The linear form of the Freundlich isotherm equation is given by Eq. (4) as follows:

$$\log q_e = \log K_f + \frac{1}{n} C_e \tag{4}$$

Figs. 13a and b show the Langmuir and Freundlich isotherm models for the adsorption of Pb(II) by PANI/OPAC. As can be seen in Table 3, the adsorption process was found to fit well to the Freundlich isotherm model (R^2 0.9688) than the Langmuir (R^2 0.9466). So that the adsorption of Pb(II) ions on the PANI/OPAC nanocomposite occurred heterogeneously. The value of 1/*n* for the adsorption of PANI/OPAC nanocomposite was 0.8169, indicating the heterogeneous nature of the adsorbent. The 1/*n* values were between 0 and 1, indicating that the biosorption of Pb(II) ions onto PANI/OPAC was favorable at studied conditions.

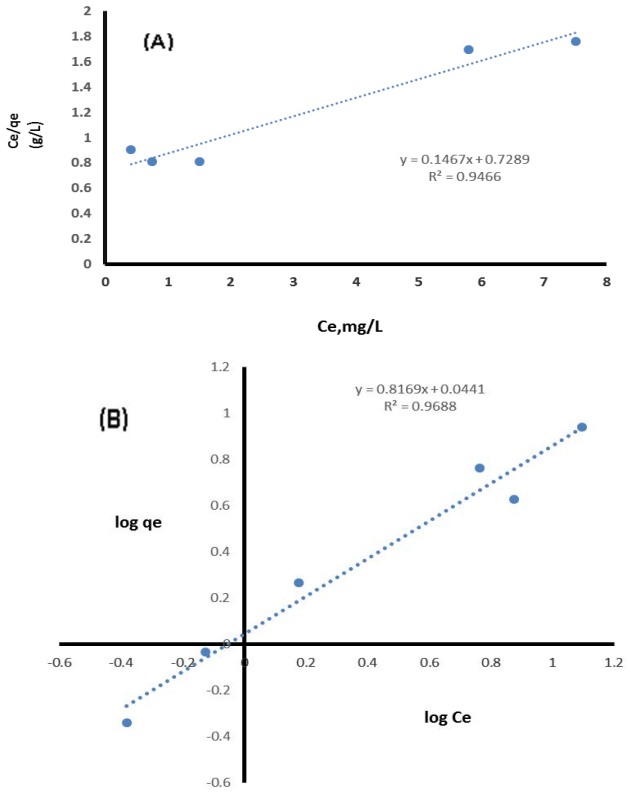

Fig. 13. (a) Langmuir isotherm and (b) Freundlich isotherm models for the adsorption of Pb(II) by PANI/OPAC.

3.6. Kinetic studies

Adsorption kinetics is important in the design and modeling of the process. of adsorption. In the present study, two kinetic models namely pseudo-first-order [46] and pseudo-second-order [47] were used to study the adsorption data of Pb(II) by PANI/OPAC as a function of time.

The pseudo-first-order equation can be expressed as:

$$\log\left(q_e - q_t\right) = \log\left(q_e\right) - \frac{K_1}{2.303}\left(t\right) \tag{5}$$

The pseudo-first-order equation can be expressed as:

$$\frac{t}{q_t} = \frac{1}{K_2 q_e^2} + \frac{1}{q_e}\left(t\right) \tag{6}$$

where q_t is the amount of PANI/OPAC adsorbed at time t (mg g^{-1}) k_1 and k_2 (g mg^{-1} min^{-1}) are the rate constants of pseudo-first-order and pseudo-second-order of adsorption of Pb(II) onto PANI/OPAC nanocomposite.

The adsorption kinetics of Pb(II) by PANI/OPAC was analyzed using pseudo-first-order and pseudo-second-order kinetic models. The application of pseudo-first-order kinetic model is not applicable for the adsorption of Pb(II) by PANI/OPAC (figure not shown). The plot of t/q_t vs. t (Fig. 14) gives a very good straight line with the correlation coefficient (0.9985). This indicates that the adsorption system studied belongs to the pseudo-second-order kinetic model. Table 4 shows the parameters of pseudo-second-order.

3.7. Adsorption thermodynamics

In this work, different thermodynamic parameters, such as the standard Gibbs free energy $\Delta G°$ (kJ mol^{-1}), the standard enthalpy ($\Delta H°$) and the standard entropy ($\Delta S°$) for biosorption of Pb(II) onto PANI/OPAC were calculated using the following equations:

$$\Delta G° = -RT \ln K_d \tag{7}$$

$$\ln K_d = \frac{\Delta S}{R} - \frac{\Delta H}{RT} \tag{8}$$

where K_d, (L g^{-1}) an equilibrium constant (Q_e/C_e), R (8.3145 KJ mol^{-1} K^{-1}) is the ideal gas constant and T (K) is the temperature.

The enthalpy ($\Delta H°$) and entropy ($\Delta S°$) were calculated from the following equation:

$$\Delta G° = \Delta H° - T\Delta S° \tag{9}$$

Table 3
Isotherm constants for the adsorption of Pb(II) on PANI/OPAC nanocomposite

Freundlich		Langmuir	
K_f	1.106	q_m (mg g^{-1})	6.81
1/*n*	0,8169	*b* (L mg^{-1})	0.201
R^2	0.9688	R^2	0.9466

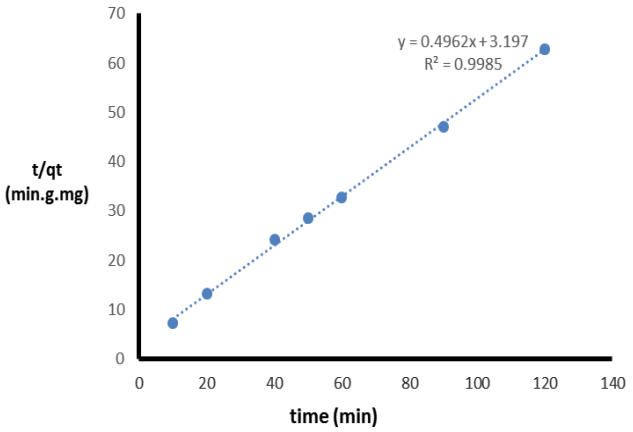

Fig. 14. Pseudo-second-order kinetic model for the adsorption of Pb(II) by PANI/OPAC.

Table 4
Kinetic parameters for the adsorption of Pb(II) on PANI/OPAC nanocomposite

Kinetic model	Parameter	Value
Pseudo-second-order	K_2 (g mg^{-1} min^{-1})	0.077
	R^2	0.9985
	q_e (mg g^{-1})	2.015

The thermodynamic parameters are given in Table 5. Fig. 15 showed the plot of ln K_d vs. 1/T, which gives a straight line with the slope of $\Delta H°/R$ and intercept of $\Delta S°/R$.

The negative value of $\Delta G°$ at three temperatures indicates the spontaneous nature of the adsorption process. Also, the $\Delta G°$ values were found to increase as the temperature increased and resulting in higher biosorption capacity. The $\Delta H°$ value was positive, indicating the endothermic nature of the biosorption of Pb(II) onto PANI/OPAC. Also, the positive values of $\Delta S°$ show increased randomness at the solid–solution interface during the biosorption process.

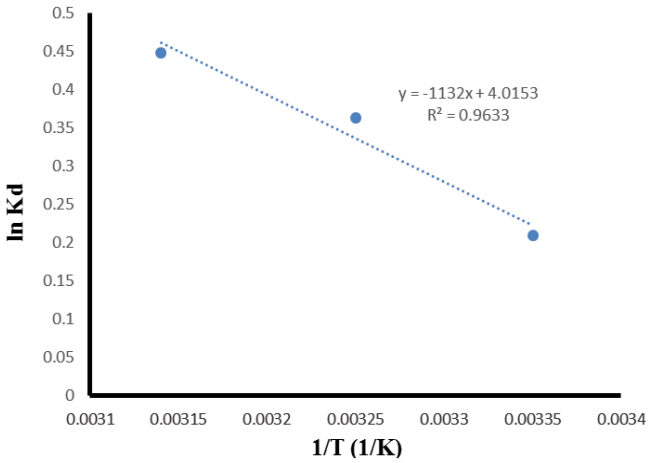

Fig. 15. Plot of ln K_d vs 1/T for the thermodynamics for adsorption of Pb(II) by PANI/OPAC.

Table 5
Thermodynamic parameters for the adsorption of Pb(II) onto PANI/OPAC nanocomposite

Temperature (K)	$-\Delta G°$ (kJ mol^{-1})	$\Delta S°$ (J mol^{-1} K^{-1})	$\Delta H°$ (kJ mol^{-1})
298	0.536		
308	0.870	33.383	9.4110
318	1.204		

3.8. Desorption and regeneration

The desorption of Pb(II) by PANI/OPAC nanocomposite was carried out by using the different desorbing agents as mentioned before. It was observed that 90.10% of Pb(II) could be desorbed by 0.1 M HCL (Fig. 16). While distilled water (5.50%) and 0.1 M EDTA (10.46%) were not efficient in the desorption of Pb(II) ions. The regeneration with HCl (desorbing agents) was considered to be more effective in desorbing heavy metals compared with other desorbing agents such as HNO_3, H_2SO_4 and NaOH [48]. The hydrogen ions from HCl easily displaced Pb(II) ions adsorbed during the desorption process by the ion-exchange process. The regeneration was repeated four cycles. Similar trends are obtained for the desorption of Pb(II) ions from activated carbon prepared from coir pith, *Eichhornia* and activated carbon cloths and pistachio shell carbon [49,50].

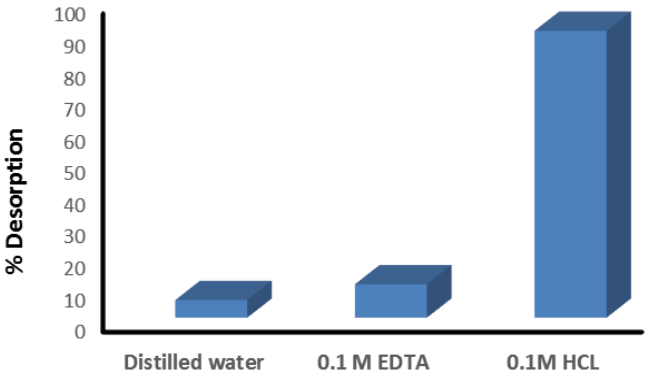

Fig. 16. Desorption of Pb(II) ions by different desorbing agents by PANI/OPAC nanocomposite.

Table 6
Comparison of the maximum adsorption capacity for Pb(II) ions by different adsorbents

Adsorbents	Q_{max} (mg g^{-1})	Metal ions	Ref.
PANI/ML	3.891	Pb(II)	[51]
PANI/JL	5.917	Pb(II)	[51]
Ash	588.24	Pb(II)	[52]
nFe-A	833.33	Pb(II)	[52]
FSAC	80.645	Pb(II)	[53]
Barley straws	23.20	Pb(II)	[54]
Coffee residue	63.29	Pb(II)	[55]
PANI/OPAC	6.81	Pb(II)	This study

3.9. Comparison of lead removal with different biosorbents

Table 6 compares the maximum adsorption capacities for PANI/OPAC nanocomposite for the adsorption of Pb(II) ions with other adsorbents. As can be seen from the table, the PANI/OPAC nanocomposite gives higher adsorption capacity than the other adsorbents [51–55].

The difference in the adsorption capacities toward lead ions depends on different parameters and experimental conditions such as adsorbent dose, temperature and pH. Also depend on BET surface area, total pore volume, functional groups and structure of the adsorbent used.

4. Conclusion

In this study, polyaniline/activated carbon composites were synthesized by in situ polymerization of aniline with APS as the oxidant in the presence of AC particles (5 wt. %), these composites were ground to nanoscale using mechanical ball mill to give PANI/ACs nanocomposites, and its ability in the removal of Pb(II) from aqueous solution was investigated. Results showed that the removal of Pb(II) ions increases with increasing solution pH and pH maximum value was at pH 4 for all the nanocomposites. By comparison between PANI, PANI/OPAC, PANI/PSAC, PANI/BPAC, PANI/ASAC and PANI/PPAC in the removal of lead, results indicated that removal efficiency of PANI/OPAC composite is higher than the other composites. Results showed that the Freundlich isotherm model better fitted the adsorption data than the Langmuir model. The kinetics of Pb(II) fitted well the pseudo-second-order kinetic model. The desorption study suggested that the PANI/OPAC can be reused successfully up to four times.

References

[1] U. Farooq, J.A. Kozinski, M.A. Khan, M. Athar, Biosorption of heavy metal ions using wheat based biosorbents—a review of the recent literature, Bioresour. Technol., 101 (2010) 5043–5053.

[2] S. Zhu, H. Hou, Y. Xue, Kinetic and isothermal studies of lead ion adsorption onto bentonite, Appl. Clay Sci., 40 (2008) 171–178.

[3] K. Zhang, WH. Cheung, M. Valix, Roles of physical and chemical properties of activated carbon in the adsorption of lead ions, Chemosphere, 60 (2004) 1129–1140.

[4] A. Sari, M. Tuzen, Kinetic and equilibrium studies of biosorption of Pb(II) and Cd (II) from aqueous solution by macrofungus (*Amanita rubescens*) biomass, J. Hazard. Mater., 164 (2009) 1004–1011.

[5] A. Saeed, M. Iqbal, M.W. Akhtar, Removal and recovery of lead (II) from single and multimetal (Cd, Cu, Ni, Zn) solutions by crop milling waste (black gram husk), J. Hazard. Mater. B, 117 (2005) 65–73.

[6] S.M. Ahmed, S.G. Mohammad, Egyptian apricot stone (*Prunus armeniaca*) as a low cost and eco-friendly biosorbent for oxamyl removal from aqueous solutions, Am. J. Exp. Agric., 4 (2014) 302–321.

[7] S.G. Mohammad, S.M. Ahmed, A.M. Badawi, A comparative adsorption study with different agricultural waste adsorbents for removal of oxamyl pesticide, Desal. Wat. Treat., 55 (2015) 2109–2120.

[8] P. Chandrasekhar, Conducting Polymers: Fundamentals and Applications—A Practical Approach, Kluwer Academic Publishers, 1999.

[9] M. Ghorbani, H. Eisazadeh, Removal of COD, color, anions and heavy metals from cotton textile wastewater by using polyaniline and polypyrrole nanocomposites coated on rice husk ash, Compos. Part B, 45 (2013) 1–7.

[10] M. Ghorbani, M. Soleimani, H. Eisazadeh, Application of polyaniline nanocomposite coated on rice husk ash for removal of Hg (II) from aqueous media, Synth. Met., 161 (2011) 1430–1433.

[11] N.A.S.A. Reyad, Using polypyrrole nanocomposites coated on rice husk ash for the removal of anions, heavy metals, COD from textile wastewater, HBRC J., 13 (2017) 297–301.

[12] M.S. Mansour, M.E. Ossman, H.A. Farag, Removal of Cd (II) ion from waste water by adsorption onto polyaniline coated on sawdust, Desalination, 272 (2011) 301–305.

[13] L. Zoleikani, H. Issazadeh, B. ZareNezhad, Preparation of new conductive polymer nanocomposites for cadmium removal from industrial wastewater, J. Chem. Technol. Metall., 50 (2015) 71–80.

[14] F. Kanwal, R. Rehman, I.Q. Bakhsh, Batch wise sorptive amputation of diamond green dye from aqueous medium by novel Polyaniline *Alstonia scholaris* leaves composite in ecofriendly way, J. Cleaner Prod., 196 (2018) 350–357.

[15] F. Kanwal, R. Rehman, J. Anwar, T. Mahmud, Adsorption studies of cadmium (II) using novel composites of polyaniline with rice husk and saw dust of *Eucalyptus camaldulensis*, Electron. J. Environ. Agric. Food Chem., 10 (2011) 2972–2985.

[16] F. Kanwal, R. Rehman,. J. Anwar; M. Saeed, Batch wise removal of chromium(VI) by adsorption on novel synthesized polyaniline composites with various brans and isothermal modeling of equilibrium data, J. Chem. Soc. Pakistan, 34 (2012) 1134–1139.

[17] F. Kanwal, R. Rehman, S. Samson, J. Anwar, Isothermal investigation of copper (II) and nickel (II) adsorption form water by novel synthesized polyaniline composites with *Polyalthia longifolia* and *Alastonia scholaris* dried leaves, Asian J. Chem., 25 (2013) 9013–9019.

[18] F. Kanwal, A. Batool, S. Rasool, S. Naseem, R. Rehman, Synthesis of polyaniline composites with grinded leaves of *Polyalthia longifolia*, *Syzygium cumini*, *Alstonia scholaris* and *Madhuca longifolia* and study of their structural, electrical and dielectric properties, Asian J. Chem., 26 (2014) 7519–7522.

[19] Mu. Naushad, T. Ahamad, G. Sharma, A.H. Al-Muhtaseb, A.B. Albadarin, M.M. Alam, Z.A. ALOthman, S.M. Alshehri, A.A. Ghfar, Synthesis and characterization of a new starch/SnO_2 nanocomposite for efficient adsorption of toxic Hg^{2+} metal ion, Chem. Eng. J., 300 (2016) 306–316.

[20] A.A. Alqadami, Mu. Naushad, M.A. Abdalla, T. Ahamad, Z.A. Alothman, S.M. Alshehri, Synthesis and characterization of Fe_3O_4@TSC nanocomposite: highly efficient removal of toxic metal ions from aqueous medium, RSC Adv., 6 (2016) 22679–22689.

[21] Mu. Naushad, Z.A. AL-Othman, M. Islam, Adsorption of cadmium ion using a new composite cation exchanger polyaniline Sn (IV) silicate: kinetics, thermodynamic and isotherm studies, Int. J. Environ Sci. Technol., 10 (2013) 567–578.

[22] D. Pathania, G. Sharma, A. Kumar, Mu. Naushad, S. Kalia, A. Sharma, Z.A. AL-Othman, Combined sorptional-photocatalytic remediation of dyes by polyaniline Zr(IV) selenotungstophosphate nanocomposite, Toxicol. Environ. Chem., 97 (2015) 526–537.

[23] F. Mashkoor, A. Nasar, Polyaniline/*Tectona grandis* sawdust: a novel composite for efficient decontamination of synthetically polluted water containing crystal violet dye, Groundwater Sustain. Dev., 8 (2019) 390–401.

[24] M. Behbahani, A. Aliakbari, M.M. Amini, A.S. Behbahani, F. Omidi, Synthesis and characterization of diphenylcarbazide-siliceous mesocellular foam and its application as a novel mesoporous sorbent for preconcentration and trace detection of copper and cadmium ions, RSC Adv., 5 (2015) 68500–68509.

[25] E. Ghorbani-Kalhor, M. Behbahani, J. Abolhasani, R.H. Khanmiri, Synthesis and characterization of modified multiwall carbon nanotubes with poly (N-phenylethanolamine) and their application for removal and trace detection of lead ions in food and environmental samples, Food Anal. Methods, 8 (2015) 1326–1334.

[26] J. Abolhasani, M. Behbahani, Application of 1-(2-pyridylazo)-2-naphthol-modified nanoporous silica as a technique in simultaneous trace monitoring and removal of toxic heavy metals in food and water samples, Environ. Monit. Assess., 187 (2015) 1–12.
[27] M.R. Nabid, R. Sedghi, M. Behbahani, B. Arvan, M.M. Heravi, H. Abdi Oskooie, Application of poly 1,8-diaminonaphthalene/multiwalled carbon nanotubes-COOH hybrid material as an efficient sorbent for trace determination of cadmium and lead ions in water samples, J. Mol. Recog., 27 (2014) 421–428.
[28] K.S.K. Reddy, A. Al Shoaibi, C. Srinivasakannan, Preparation of porous carbon from date palm seeds and process optimization, Int. J. Environ. Sci. Technol., 12 (2015) 959–966.
[29] V.O. Njoku, B.H. Hameed, Preparation and characterization of activated carbon from corncob by chemical activation with H_3PO_4 for 2, 4-dichlorophenoxyacetic acid adsorption, Chem. Eng. J., 173 (2011) 391–399.
[30] H. Zengin, G. Kalayc, Synthesis and characterization of polyaniline/activated carbon composites and preparation of conductive films, Mater. Chem. Phys., 120 (2010) 46–53.
[31] F.N. Arslanoglu, F. Kar, N. Arslan, Adsorption of dark coloured compounds from peach pulp by using powdered activated carbon, J. Food Eng., 71 (2005) 156–163.
[32] N. Li, S. Deng., G. Yu, J. Huang, Efficient removal of Cu (II), Pb(II), Cr (VI) and As (V) from aqueous solution using an aminated resin prepared by surface-initiated atom transfer radical polymerization, Chem. Eng. J., 165 (2010) 751–757.
[33] F. Kanwal, R. Rehman, T. Mahmud, J. Anwar, R. Ilyas, Isothermal and thermodynamical modeling of chromium (III) adsorption by composites of polyaniline with rice husk and saw dust, J. Chilean Chem. Soc., 57 (2012) 1058–1063.
[34] K. Kumar, R.K. Saxena, R.D. Kothari, K. Suri, N.K. Kaushik, J.N. Bohra, Correlation between adsorption and x-ray diffraction studies on viscose rayon based activated carbon cloth, Carbon, 35 (1997) 1842–1844.
[35] A.K. Aboul-Gheit, S.M. Ahmed, D.S. El-Desouki, N.E. Moustafa, S.M. Abdel-Azeem, Nanocrystalline Pt/TiO_2 Catalysts for 4-chlorophenol photocatalytic degradation, Egypt. J. Petrol., 19 (2010) 45–58.
[36] J.Z. Lyu, L.Z. Zhu, C. Burda, Optimizing nanoscale TiO_2 for adsorption-enhanced photocatalytic degradation of low-concentration air pollutants, ChemCatChem., 5 (2013) 3114–3123.
[37] P.C. Ramamurthy, A.M. Malshe, W.R. Harrell, R.V. Gregory, K. McGuire, A.M. Rao, Polyaniline/single-walled carbon nanotube composite electronic devices, Solid State Electron., 48 (2004) 2019–2024.
[38] F.Y. Chuang, S.M. Yang, Cerium dioxide/polyaniline core-shell nanocomposites, J. Colloid Interface Sci., 320 (2008) 194–201.
[39] M. Kula, H. Karaoglu, A. Celik, Adsorption of Cd (II) ions from aqueous solutions using activated carbon prepared from olive stone by $ZnCl_2$ activation, Bioresour. Technol., 99 (2008) 492–501.
[40] S.T. Atkar, S. Arslan, T. Alp, D. Arslan, T. Akar, Biosorption potential of the waste biomaterial obtained from *Cucumis melo* for the removal of Pb^{2+} ions from aqueous media: equilibrium, kinetic and thermodynamic and mechanism analysis, Chem. Eng., 185–186 (2010) 82–90.
[41] D.N. Olowoyo, A.O. Garuba, Adsorption of cadmium ions using activated carbon prepared from coconut shell, global advanced research, J. Food Sci. Technol., 1 (2012) 81–84.
[42] I. Langmuir, The adsorption of gases on plane surfaces of glass, mica and platinum, J. Am. Chem. Soc., 40 (1918) 1361–1403.
[43] H. Freundlich, U¨ber die adsorption in lo¨sungen [Adsorption in solution], Z. Phys. Chem., 57 (1906) 370–384.
[44] A. Rostami, M.A. Anbaz, H.E. Gahrooei, M. Arabloo, A. Bahadori, Accurate estimation of CO_2 adsorption on activated carbon with multi-layer feed-forward neural network (MLFNN) algorithm, Egypt. J. Petrol., 27 (2018) 65–73.
[45] M.A.M. Salleh, D.K. Mahmoud, W.A. Karim, A. Idris, Cationic and anionic dye adsorption by agricultural solid wastes: a comprehensive review, Desalination, 280 (2011) 1–13.
[46] J. Febrianto, A.N. Kosasih, J. Sunarso, Y.-H. Ju, N. Indraswati, S. Ismadji, Equilibrium and kinetic studies in adsorption of heavy metals using biosorbent: a summary of recent studies, J. Hazard. Mater., 162 (2009) 616–645.
[47] M. Özacar, I.A. Sengil, A two stage batch adsorbed design for methylene blue removal to minimize contact time, J. Environ. Manage., 80 (2006) 372–379.
[48] E. Maranon, H. Sastre, Preconcentration and removal of trace metals from water by apple waste, Bioresour. Technol., 40 (1992) 73–76.
[49] P. Shekinah, K. Kadirvelu, P. Kanmani, P. Senthilkumar, V. Subburam, Adsorption of Lead (II) from aqueous solution by activated carbon prepared from *Eichhornia*. J. Chem. Technol. Biotechnol., 77 (2002) 1–7.
[50] H.S. Shaziya, A. Rais, Pistachio Shell Carbon (PSC) – an agricultural adsorbent for the removal of Pb(II) from aqueous solution, Groundwater Sustain. Dev., 4 (2017) 42–48.
[51] F. Kanwal, R. Rehman, J. Anwar, S. Rasul, Adsorptive Removal of Pb(II) from Water Using Novel Synthesized Polyaniline Composites with *Madhuca longifolia* and *Eugenia jambolana* Leaf Powder, Asian J. Chem., 26 (2014) 4963–4967.
[52] M. Ghasemi, Mu. Naushad, N. Ghasem, Y. Khosravi-fard, Adsorption of Pb(II) from aqueous solution using new adsorbents prepared from agricultural waste: adsorption isotherm and kinetic studies, J. Ind. Eng. Chem., 20 (2014) 2193–2199.
[53] M. Ghasemi, Mu. Naushad, N. Ghasemi, Y. Khosravi-fard, A novel agricultural waste based adsorbent for the removal of Pb(II) from aqueous solution: kinetics, equilibrium and thermodynamic studies, J. Ind. Eng. Chem., 20 (2014) 454–461,
[54] E. Pehlivan, T. Altun, S. Parlayici, Utilization of barley straws as biosorbents for Cu^{2+} and Pb^{2+} ions, J. Hazard. Mater., 164 (2009) 982–986.
[55] F. Boudrahem, F. Aissani-Benissad, H. Aït-Amar, Batch sorption dynamics and equilibrium for the removal of lead ions from aqueous phase using activated carbon developed from coffee residue activated with zinc chloride, J. Environ. Manage., 90 (2009) 3031–3039.